

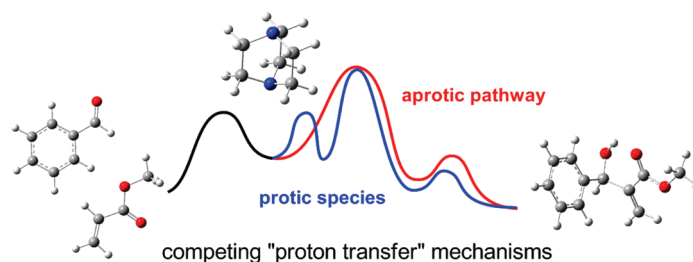
## A Unified Mechanistic View on the Morita–Baylis–Hillman Reaction: Computational and Experimental Investigations

David Cantillo\*<sup>†</sup> and C. Oliver Kappe\*

Christian Doppler Laboratory for Microwave Chemistry (CDLMC) and Institute of Chemistry, Karl-Franzens-University Graz, Heinrichstrasse 28, A-8010 Graz, Austria. <sup>†</sup>On leave from the Departamento de Química Orgánica e Inorgánica, QUOREX Research Group, Facultad de Ciencias, Universidad de Extremadura, E-06006 Badajoz, Spain

dcannie@unex.es; oliver.kappe@uni-graz.at

Received October 22, 2010



The thermodynamic properties and reaction mechanism of the Morita–Baylis–Hillman (MBH) reaction have been investigated through experimental and computational techniques. The impossibility to accelerate this synthetically valuable transformation by increasing the reaction temperature has been rationalized by variable-temperature experiments and MP2 theoretical calculations of the reaction thermodynamics. An increase in temperature results in a switching of the equilibrium to the reactants occurring at even moderate temperature levels. The complex reaction mechanism for the MBH reaction has been investigated through an in-depth analysis of the suggested alternative pathways, using the M06-2X computational method. The results provided by this theoretical approach are in agreement with all the experimental/kinetic evidence such as reaction order, acceleration by protic species (methanol, phenol), and autocatalysis. In particular, the existing controversy about the character of the key proton transfer in the MBH reaction (Aggarwal versus McQuade pathways) has been resolved. Depending on the specific reaction conditions both suggested pathways are competing mechanisms, and depending on the amount of protic species and the reaction progress (early or late stage) either of the two mechanisms will be favored.

### Introduction

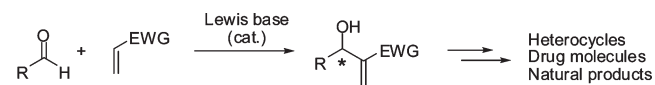
The Morita–Baylis–Hillman (MBH) reaction is arguably one of the most powerful and versatile carbon–carbon bond forming methods in organic synthesis.<sup>1,2</sup> In this catalytic

reaction between a carbonyl-based electrophile and a Michael acceptor densely functionalized products containing a new stereocenter can be obtained in a single-step operation without generating any waste or byproducts (Scheme 1). Because of its atom economic nature, the utilization of relatively simple starting materials, and its comparatively wide substrate scope, this carbon–carbon bond forming protocol has found numerous applications in synthetic organic chemistry in the past two decades, including the development of asymmetric and intramolecular versions.<sup>1,2</sup>

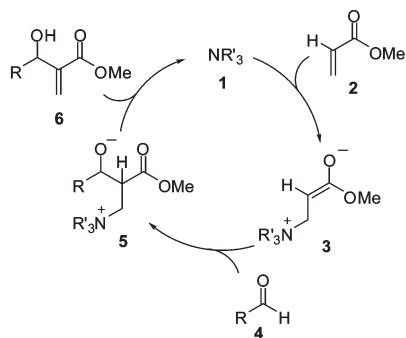
Despite the fact that the MBH reaction has been first described more than 40 years ago,<sup>3</sup> there is still an ongoing debate in the scientific community on the exact reaction mechanism and the kinetics of this important synthetic

(1) For a recent review with more than 1000 references on the MBH reaction, see: Basavaiah, D.; Reddy, B. S.; Badsara, S. S. *Chem. Rev.* **2010**, *110*, 5447–5674.

(2) For other selected reviews, see: (a) Basavaiah, D.; Rao, K. V.; Reddy, R. J. *Chem. Soc. Rev.* **2007**, *36*, 1581–1588. (b) Masson, G.; Housseman, C.; Zhu, J. *Angew. Chem., Int. Ed.* **2007**, *46*, 4614–4628. (c) Basavaiah, D.; Rao, J. A.; Satyanarayana, T. *Chem. Rev.* **2003**, *103*, 811–891. (d) Langer, P. *Angew. Chem., Int. Ed.* **2000**, *39*, 3049–3052. (e) Ciganek, E. In *Organic Reactions*; Paquette, L. A., Ed.; Wiley: New York, 1997; Vol. 51, pp 201–350. (f) Basavaiah, D.; Rao, P. D.; Hyma, R. S. *Tetrahedron* **1996**, *52*, 8001–8062. (g) Drewes, S. E.; Roos, G. H. P. *Tetrahedron* **1988**, *44*, 4653–4670.

**SCHEME 1. The Morita–Baylis–Hillman (MBH) Reaction and the General Reaction Mechanism Proposed by Hill and Isaacs**


R = alkyl or aryl  
EWG = CO<sub>2</sub>R, CHO, CN, COR, etc.



transformation.<sup>4–13</sup> While the global mechanistic sequence and catalytic cycle shown in Scheme 1 first suggested by Hill and Isaacs in the late 1980s is widely accepted today,<sup>4</sup> the current discussion is focusing on the mechanism of the proton 1,3-shift and the nature of the rate-determining step (RDS). On the basis of the initial attempts to shed light on the reaction mechanism through kinetic studies by Hill and Isaac,<sup>4</sup> the proposed RDS was assumed to be the carbon–carbon bond formation in the aldolic addition reaction of the zwitterionic amine–acrylate adduct **3** and an aldehyde molecule **4**. This proposal was supported by subsequent independent investigations including the interception of all key intermediates using electrospray ionization with mass and tandem mass spectrometry<sup>5</sup> and X-ray analysis of one of the intermediates in the catalytic cycle (**3**).<sup>6</sup>

However, more recently the groups of McQuade<sup>7</sup> and Aggarwal<sup>8</sup> reinvestigated the kinetics of the MBH reaction by means of the kinetic isotope effect (KIE) employing an  $\alpha$ -<sup>2</sup>H acrylate precursor and proposed the RDS to be the proton transfer step **5** → **6**. In the above-mentioned experiments Aggarwal also observed that the reaction shows

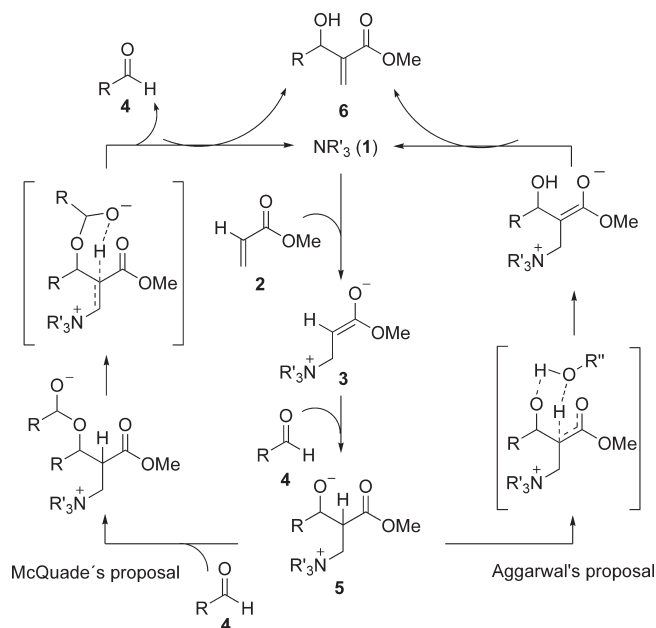


**FIGURE 1.** Current mechanistic proposals for the Morita–Baylis–Hillman (MBH) reaction.

autocatalysis after approximately 20% conversion,<sup>8</sup> while McQuade observed a second-order character for the aldehyde in the reaction.<sup>7</sup> On the basis of these experimental findings two new mechanistic hypotheses were proposed as outlined in Figure 1. The viewpoints differ in the manner in which the hydrogen migration takes place, and to date this question has not been fully resolved. In fact, recent electrospray ionization mass spectrometry studies provide strong experimental evidence that both mechanisms are possible.<sup>9</sup>

The ongoing debate about the character of the key pathways and transition states prompted Aggarwal and Harvey to perform a detailed computational study on the MBH reaction.<sup>10</sup> In their work, the role of the alcohol species (methanol) along with the mechanism proposed by McQuade with a second-order kinetics for the aldehyde were discussed. However, these theoretical investigations could not completely address all the known experimental findings in the MBH reaction, such as the observed second-order kinetics for the reaction even in the presence of protic solvents<sup>7</sup> (which was hypothesized by Aggarwal and Harvey to be the result of different aldehyde reactivities), or the important influence of temperature on the reaction thermodynamics.<sup>1,2</sup> In our opinion, these open points are likely to be the result of the recently discovered extremely poor performance of the chosen computational method (B3LYP) in predicting the barrier heights for the MBH reaction,<sup>11</sup> and the lack of vibrational analysis that only allows an estimate of free energies.

Apart from the Aggarwal/Harvey investigation mentioned above,<sup>10</sup> a few additional computational studies recently appeared in the literature attempting to address mechanistic questions in the MBH reaction, including the addition of explicit water or methanol molecules.<sup>12</sup> However, in all these studies the inappropriate B3LYP method was used, or potential electronic energies were employed to describe the energetics instead of the more adequate free energies.<sup>12</sup> In this context, it should be mentioned that the theoretical approach of Sunoj,<sup>13</sup> who employed CBS-4 M and mPW1K

(3) (a) Morita, K.; Suzuki, Z.; Hirose, H. *Bull. Chem. Soc. Jpn.* **1968**, *41*, 2815–2815. (b) Baylis, A. B.; Hillman, M. E. D. German Patent 2155113, 1972; *Chem. Abstr.* **1972**, *77*, 34174q.

(4) (a) Hill, J. S.; Isaacs, N. S. *J. Phys. Org. Chem.* **1990**, *3*, 285–288. (b) Hill, J. S.; Isaacs, N. S. *J. Chem. Res.* **1988**, 330. (c) Hill, J. S.; Isaacs, N. S. *Tetrahedron Lett.* **1996**, *27*, 5007–5010.

(5) Santos, L. S.; Pavam, C. H.; Almeida, W. P.; Coelho, F.; Eberlin, M. N. *Angew. Chem., Int. Ed.* **2004**, *43*, 4330–4333.

(6) Drewes, E.; Njamela, O. L.; Emslie, N. D.; Ramesar, N.; Field, J. S. *Synth. Commun.* **1993**, *23*, 2807–2815.

(7) (a) Price, K. E.; Broadwater, S. J.; Jung, H. M.; McQuade, D. T. *Org. Lett.* **2005**, *7*, 147–150. (b) Price, K. E.; Broadwater, S. J.; Walker, B. J.; McQuade, D. T. *J. Org. Chem.* **2005**, *70*, 3980–3987.

(8) Aggarwal, V. K.; Fulford, S. Y.; Lloyd-Jones, G. C. *Angew. Chem., Int. Ed.* **2005**, *44*, 1706–1708.

(9) Amarante, G. W.; Milagre, H. M. S.; Vaz, B. G.; Ferreira, B. R. V.; Eberlin, M. N.; Coelho, F. *J. Org. Chem.* **2009**, *74*, 3031–3037.

(10) Robiette, R.; Aggarwal, V. K.; Harvey, J. N. *J. Am. Chem. Soc.* **2007**, *129*, 15513–15525.

(11) Harvey, J. N. *Faraday Discuss.* **2010**, *145*, 487–505.

(12) (a) Xu, J. J. *THEOCHEM* **2006**, *767*, 61–66. (b) Li, J. J. *Theor. Comput. Chem.* **2010**, *9*, 65–75. (c) Jian-Fen, F.; Chun-Hong, Y.; Liang-Jun, H. *Int. J. Quantum Chem.* **2009**, *109*, 1311–1321. (d) Dong, L.; Qin, S.; Su, Z.; Yang, H.; Hu, C. *Org. Biomol. Chem.* **2010**, *8*, 3985–3991.

(13) (a) Roy, D.; Sunoj, R. B. *Org. Lett.* **2007**, *9*, 4873–4876. (b) Roy, D.; Sunoj, R. B. *Chem.—Eur. J.* **2008**, *14*, 10530–10534. (c) Roy, D.; Patel, C.; Sunoj, R. B. *J. Org. Chem.* **2009**, *74*, 6936–6943.

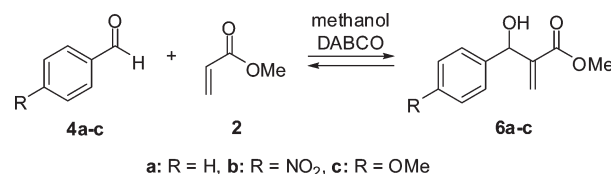
methods to compute the free energy barriers for the reaction, is interesting but only compares the energetics of the direct proton transfer pathways (via a four-membered transition structure) and the proton 1,3-shift assisted by water, omitting the possibility of the assistance by a second molecule of aldehyde or other protic species.

In the present work we present a detailed computational and experimental reinvestigation on the amine-catalyzed MBH reaction of benzaldehyde with methyl acrylate. In particular, issues relating to the hitherto neglected temperature dependence of the thermodynamic properties—which prevents the use of elevated temperatures as an activation method in the otherwise sluggish MBH reaction—are addressed. In addition, we computationally reinvestigate, employing the recently introduced M06-2X method<sup>14</sup> that provides accurate thermodynamics for carbon–carbon bond forming reactions,<sup>15</sup> all the previously suggested mechanistic proposals for this transformation, emphasizing the most controversial step: the proton migration from the  $\alpha$ -carbon to the oxygen derived from the aldehyde counterpart (Figure 1). To fully address the mechanistic conundrum surrounding the MBH reaction, we also take into consideration the reagents/additives reported in the literature to activate this proton migration step: a second molecule of aldehyde,<sup>7</sup> alcohols,<sup>16</sup> water,<sup>16,17</sup> phenol,<sup>18</sup> and the observed autocatalysis.<sup>8</sup> Grati-fyingly, these new calculations can rationalize all existing experimental evidence, and most importantly, can settle the argument about the character of the hydrogen migration step, in particular the Aggarwal versus McQuade proposals (Figure 1). On the basis of the present theoretical study and a reinterpretation of the available kinetic data it can be concluded that both mechanisms are competing reactions, and depending on the reaction progress and conditions either of the two pathways is favored.

### Computational Details

All geometries and energies, as well as frequency calculations, were computed with use of the Gaussian09 package.<sup>19</sup> The MP2<sup>20</sup> method along with the 6-311+G(d,p) basis set was employed for the temperature dependence studies. In the case of the pathway simulations, the M06-2X<sup>14</sup> density-functional method with the 6-311G(d,p) basis was used.<sup>21</sup> The geometries were optimized including the solvation effect. For this purpose the SMD<sup>22</sup> solvation method was employed, using methanol or tetrahydrofuran as solvent. The frequency calculations on all the stationary points were carried out at the same level of theory as the geometry optimizations to ascertain the nature of the

### SCHEME 2. The DABCO-Catalyzed Morita–Baylis–Hillman (MBH) Reaction of Aryl Aldehydes (**4**) with Methyl Acrylate (**2**)



stationary points. Ground and transition states were characterized by none and one imaginary frequencies, respectively.

All the presented relative energies are free energies with respect to the reactants. As in previous studies,<sup>7,8,10,13</sup> the reaction of benzaldehyde with methyl acrylate and DABCO was chosen as the model for the MBH reaction. In addition, 4-nitrobenzaldehyde and 4-methoxybenzaldehyde were also employed in order to observe substituent effects in the temperature dependence studies. Since along the mechanistic pathways several diastereomeric transition structures can be formed, all the possibilities have been investigated and are presented in the Supporting Information.

### Results and Discussion

#### Temperature Dependence of Thermodynamic Properties.

For the present study we have chosen the reaction between benzaldehyde (**4a**) and methyl acrylate (**2**) catalyzed by diazabicyclo[2.2.2]octane (DABCO) (**1**) in methanol as the model system, since this reaction can be considered the archetypal MBH reaction and is one of the most experimentally studied examples (Scheme 2).<sup>1–10</sup> The most relevant experimental and theoretical mechanistic studies on the MBH reaction by McQuade<sup>7</sup> and Aggarwal<sup>8,10</sup> were also carried out with this system. Additional experimental data with 4-nitrobenzaldehyde (**4b**) instead of benzaldehyde have also been reported.<sup>7</sup>

The available computational data on this transformation, with similar energies for the reactants and the product, point to a reversible character for the MBH reaction.<sup>10</sup> However, in a previous study<sup>7</sup> attempts to experimentally observe the reversibility of this model reaction (the reaction of **4a** was chosen in this study) were unsuccessful. To clarify this issue for our model system, a purified sample of MBH adduct **6a** was resubjected to the reaction conditions. After dissolving adduct **6a** in methanol in the presence of DABCO (2 equiv) and heating the mixture at 120 °C for 1 h the formation of aldehyde substrate **4a** in considerable amounts (~68% by GC-FID) was observed. Importantly, by letting the reaction mixture stand at room temperature and monitoring the progress continuously by GC-FID the equilibrium again shifted to the product side, with 72% MBH adduct **6a** being observable after 24 h. These simple experimental studies not only verify the reversible character of the MBH reaction, but also point to a strong temperature dependence of the equilibrium constant, in the sense that the adduct (**6a**) is favored at low temperatures, while the reactants **4a** + **2** are the major species at elevated temperatures.

This temperature dependence can in principle be observed in computational studies on the MBH reaction. In the previous theoretical study by Aggarwal and Harvey<sup>10</sup> no frequency analysis of the stationary points is presented, thus avoiding the chance to determine any temperature influence.

(14) Zhao, Y.; Truhlar, D. G. *Theor. Chem. Acc.* **2008**, *120*, 215–241.

(15) Pieniazek, S. N.; Clemente, F. R.; Houk, K. N. *Angew. Chem., Int. Ed.* **2008**, *47*, 7746–7749.

(16) Aggarwal, V. K.; Emme, I. S.; Fulford, Y. *J. Org. Chem.* **2003**, *68*, 692–700.

(17) Cai, J.; Zhou, Z.; Zhao, G.; Tang, C. *Org. Lett.* **2002**, *4*, 4723–4725.

(b) Aggarwal, V. K.; Dean, D. K.; Mereu, A.; Williams, R. *J. Org. Chem.* **2002**, *67*, 510–514.

(18) Faltin, C.; Fleming, E. M.; Connon, S. J. *J. Org. Chem.* **2004**, *69*, 6496–6499.

(19) *Gaussian 09*, Revision A.1; Frisch, M. J. et al.; Gaussian, Inc., Wallingford, CT, 2009.

(20) Head-Gordon, M.; Pople, J. A.; Frisch, M. J. *J. Chem. Phys. Lett.* **1988**, *153*, 503–506.

(21) Single points calculations for key transition structures with the 6-311+G(d,p) basis set were also performed to ensure that the addition of diffuse functions does not affect the drawn conclusions.

(22) Marenich, A. V.; Cramer, C. J.; Truhlar, D. G. *J. Phys. Chem. B* **2009**, *113*, 6378–6396.

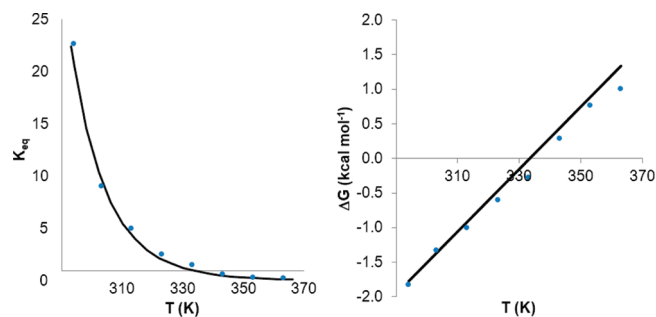


**FIGURE 2.** Theoretical (line) and experimental (dots) temperature dependence of the equilibrium constant  $K_{eq}$  (left) and free energy  $\Delta G$  (right) in the MBH reaction of benzaldehyde (**4a**) with methyl acrylate (**2**) (Scheme 2).

The Sunoj<sup>13</sup> theoretical work employs free energies, but focuses on the reaction energy barriers omitting the energetics of the global process. The DFT method used in most of the above-mentioned papers is B3LYP.<sup>23</sup> This DFT method along with the 6-311+G(d,p) basis set and the SMD solvation method (using methanol as solvent) predicts a reaction free energy of +14.4 kcal mol<sup>-1</sup> at 298.15 K for the MBH reaction **4a** + **2** → **6a** (Scheme 2). This is obviously incorrect since the reaction is spontaneous at room temperature. This erroneous energetics along with previous observations<sup>11</sup> about the energy barriers computed with this DFT method clearly reveal the inadequacy of the B3LYP approach to model the MBH reaction.

To understand the temperature influence in the MBH thermodynamics a more accurate computational approach is therefore required. For the present work the ab initio method MP2, with the 6-311+G(d,p) basis set was selected. The geometries were optimized including the solvent effect (SMD model, methanol as solvent). At this theoretical level we obtained the theoretical enthalpy and entropy of reaction, -15.0 kcal mol<sup>-1</sup> and -45.01 cal mol<sup>-1</sup> K<sup>-1</sup>, respectively. With these data we were able to display the dependence of free energy of reaction  $\Delta G$  and of the equilibrium constant  $K_{eq}$  with the temperature, as depicted in the Figure 2.

Noticeably, above approximately 330 K (57 °C) the reaction becomes endergonic, providing a rationalization for the fact that MBH reactions generally cannot be performed at elevated temperatures.<sup>1,2</sup> To further confirm this hypothesis experimentally, we carried out the reaction shown in Scheme 2 at different temperatures ranging from 293 to 383 K (20–90 °C) (above this temperature range it is difficult to avoid the decomposition of the DABCO catalyst and the polymerization of methyl acrylate). The different equilibrium constants were obtained (a detailed description can be found in the Experimental Section and the Supporting Information) taking data points from 3 h to 7 d using GC-FID monitoring, and from these values the experimental enthalpy and entropy of reaction were calculated. These resulting values were  $\Delta H = -13.94$  kcal mol<sup>-1</sup> and  $\Delta S = -41.3$  cal mol<sup>-1</sup> K<sup>-1</sup>. The experimental plots (Figure 2) show endergonic reactions above approximately 330 K (57 °C), as the ab initio calculations predicted, and experimental thermodynamic properties very close to the MP2 theoretical values.

In principle, the fact that the equilibrium constant of a chemical reaction can be temperature dependent is well-known.<sup>24</sup> The switch of  $\Delta G$  from exergonic to endergonic (negative to positive), which turns  $K > 1$ , occurs at a temperature given by eq 1. The MBH reaction is somewhat unusual since its enthalpy and entropy values in eq 1 result in a switch to endergonic reaction near room temperature ( $\Delta H/\Delta S \approx 330$  K). This coincidence results in a rare inversion of the equilibrium when increasing the temperature even slightly.

$$\Delta H - T \cdot \Delta S = 0 \Rightarrow T = \frac{\Delta H}{\Delta S} \quad (1)$$

The MBH reaction with 4-nitrobenzaldehyde (**4b**) as starting material presents an interesting case since this substrate has also been widely used in the MBH reaction,<sup>1,2</sup> including the McQuade kinetic studies on the reaction mechanism.<sup>7</sup> In addition, some authors have shown that using 4-nitrobenzaldehyde as a substrate the reaction can be heated (for example, using microwave dielectric heating),<sup>25</sup> which points to a likely change in the temperature effect.<sup>1,2</sup> Therefore, similar experiments and calculations were performed with 4-nitrobenzaldehyde (**4b**) and methyl acrylate (**2**) under otherwise identical conditions. Figure 3 shows a comparison between the experimental temperature dependence of the equilibrium constants and free energies for the MBH reactions with benzaldehyde (**4a**) and 4-nitrobenzaldehyde (**4b**) as substrates. The difference in thermodynamic properties between the two substrates confirms the possibility of carrying out MBH reactions with 4-nitrobenzaldehyde (**4b**) at higher temperatures, as this process becomes endergonic only at temperatures above approximately 380 K (107 °C). This suggests that using, for an example, an excess of acrylate **2**, comparatively high conversions can be achieved even at elevated temperatures.<sup>1,2</sup>

To further confirm the suitability of the selected ab initio method for these investigations, we also calculated the theoretical plot for the temperature dependence for the 4-nitrobenzaldehyde reaction at the same level of theory (Figure 4). In addition, the data for 4-methoxybenzaldehyde (**4c**), which could not be experimentally accessed because of the exceedingly long reaction times, are also included. As expected, the theoretical plot for the 4-nitrobenzaldehyde reaction is displaced to higher temperatures with respect to benzaldehyde in agreement with the experimental data (cf. Figure 3). For 4-methoxybenzaldehyde the calculations indicate the opposite effect and thus an unfavored reaction. This explains the low conversions and yields obtained with electron-donor substrates, and reveals the endergonic character of these MBH reactions even at moderate temperatures.<sup>1,2</sup>

Since the MBH reaction is known to be rather sluggish generally requiring long reaction times, interest in the past decades has focused on methods to accelerate this synthetically very useful process.<sup>1,2</sup> In the context of our temperature-dependence studies, the use of microwave irradiation is particularly interesting. Since the proposed mechanism for the MBH reaction involves a series of polar (zwitterionic) intermediates (Figure 1) the possibility of the involvement of

(24) Atkins, P.; de Paula, J. In *Physical Chemistry for the Life Sciences*, 1st ed.; W.H. Freeman: New York, 2005; Chapter 4, pp 151–199.

(25) For a review on microwave-assisted MBH reactions, see: De Souza, R. O. M. A.; Miranda, L. S. M. *Mini Rev. Org. Chem.* **2010**, *7*, 212–220.

(23) (a) Becke, A. D. *J. Chem. Phys.* **1993**, *98*, 5648–5652. (b) Lee, C.; Yang, W.; Parr, R. G. *Phys. Rev. B* **1988**, *37*, 785–789.

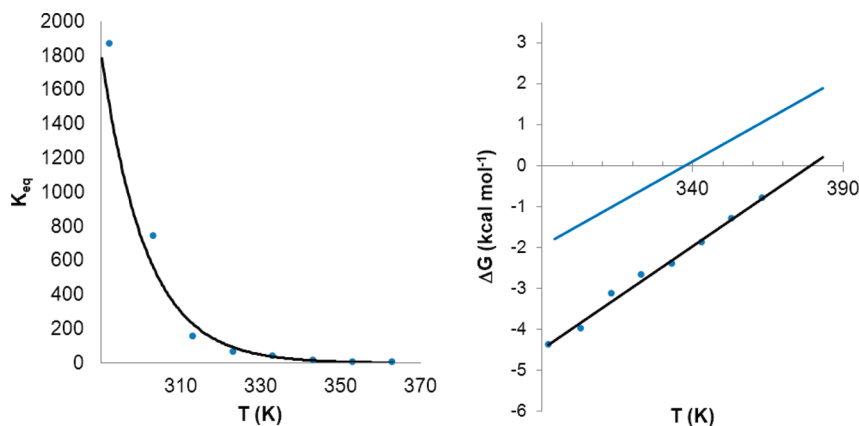


**FIGURE 3.** Experimental temperature dependence of the equilibrium constant  $K_{eq}$  (left) and the free energy  $\Delta G$  (right) in the MBH reaction of 4-nitrobenzaldehyde (**4b**) with methyl acrylate (**2**) (Scheme 2). For comparison purposes, the experimental free energy data for benzaldehyde (**4a**) (cf. Figure 2) are also shown (blue line). Experimental thermodynamic data for 4-nitrobenzaldehyde (**4b**):  $\Delta H = -19.01$  kcal mol $^{-1}$  and  $\Delta S = -50.1$  cal mol $^{-1}$  K $^{-1}$ .

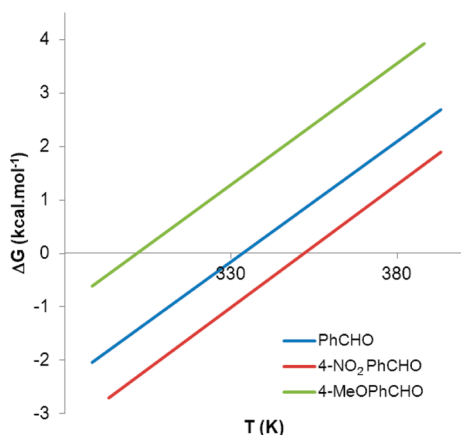


**FIGURE 4.** Comparison of theoretical temperature dependence on the free energies  $\Delta G$  for the MBH reaction with benzaldehyde (**4a**), 4-nitrobenzaldehyde (**4b**), and 4-methoxybenzaldehyde (**4c**) as substrates (Scheme 2). Computed (MP2) thermodynamic data: 4-nitrobenzaldehyde (**4b**):  $\Delta H = -16.18$  kcal mol $^{-1}$  and  $\Delta S = -46.0$  cal mol $^{-1}$  K $^{-1}$ ; 4-methoxybenzaldehyde (**4c**) (MP2):  $\Delta H = -13.7$  kcal mol $^{-1}$  and  $\Delta S = 45.4$  cal mol $^{-1}$  K $^{-1}$ .

so-called nonthermal microwave effects, stabilizing these intermediates (or transition states) cannot be ruled out.<sup>26,27</sup> Essentially, nonthermal microwave effects have been postulated to result from a proposed direct interaction of the electric field with specific molecules in the reaction medium that is not related to a macroscopic temperature effect. It has been argued, for example, that the presence of an electric field leads to orientation effects of dipolar molecules or intermediates and hence changes the pre-exponential factor  $A$  or the activation

energy (entropy term) in the Arrhenius equation for certain types of reactions.<sup>27</sup> Furthermore, a similar effect has been proposed for polar reaction mechanisms, where the polarity is increased going from the ground state to the transition state, resulting in an enhancement of reactivity by lowering the activation energy.<sup>27</sup> Specific microwave effects have been suggested for a wide variety of synthetic transformations,<sup>27</sup> including for the MBH reaction.<sup>25</sup>

To establish if nonthermal microwave effects are involved in MBH reactions carried out in a microwave field,<sup>25</sup> we have repeated the experiments involving benzaldehyde as substrate described above using a single-mode microwave reactor<sup>28</sup> instead of a standard conductive heating method. When using internal temperature monitoring employing a fiber-optic probe to ensure that accurate reaction temperatures are obtained,<sup>29</sup> no difference in the kinetic data compared to standard conductive heating was obtained.<sup>30</sup> In addition, to ensure that the electric field component of the microwave irradiation has no effect on the reaction energetics, we also included a field of  $10^5$  V m $^{-1}$  into the theoretical calculations, a field strength that is approximately 10 times higher than that typically attained in a commercial single-mode microwave reactor.<sup>31</sup> Since very small changes are expected in the thermodynamic properties of the reaction when including an electric field of this strength, we improved the default accuracy of the Gaussian09 software in order to detect these very small changes. Thus, the SCF convergence criteria were set to  $10^{-10}$  atomic units, and the 2-electron integral accuracy parameter was set to  $10^{-14}$ . The “NoVarAcc” keyword was also included in order to switch to full integral accuracy in the SCF calculation. Table 1 collects the

(26) For a more detailed definition and examples for thermal, specific, and nonthermal microwave effects, see: (a) Kappe, C. O. *Angew. Chem., Int. Ed.* **2004**, *43*, 6250. (b) Kappe, C. O.; Dallinger, D.; Murphree, S. S. *Practical Microwave Synthesis for Organic Chemists—Strategies, Instruments, and Protocols*; Wiley-VCH: Weinheim, Germany, 2009; pp 20–44.

(27) For leading reviews on microwave effects, see: (a) Perreux, L.; Loupy, A. *Tetrahedron* **2001**, *57*, 9199. (b) Perreux, L.; Loupy, A. In *Microwaves in Organic Synthesis*; Loupy, A., Ed.; Wiley-VCH: Weinheim, Germany, 2002; Chapter 3, pp 61–114. (c) Perreux, L.; Loupy, A. In *Microwaves in Organic Synthesis*, 2nd ed.; Loupy, A., Ed.; Wiley-VCH: Weinheim, Germany, 2006; Chapter 4, pp 134–218. (d) De La Hoz, A.; Diaz-Ortiz, A.; Moreno, A. *Chem. Soc. Rev.* **2005**, *34*, 164. (e) De La Hoz, A.; Diaz-Ortiz, A.; Moreno, A. In *Microwaves in Organic Synthesis*, 2nd ed.; Loupy, A., Ed.; Wiley-VCH: Weinheim, Germany, 2006; Chapter 5, pp 219–277.

(28) (a) Obermayer, D.; Gutmann, B.; Kappe, C. O. *Angew. Chem., Int. Ed.* **2009**, *48*, 8321–8342. (b) Gutmann, B.; Obermayer, D.; Reichart, B.; Prekodravac, B.; Irfan, M.; Kremsner, J. M.; Kappe, C. O. *Chem.—Eur. J.* **2010**, *16*, 12182–1294.

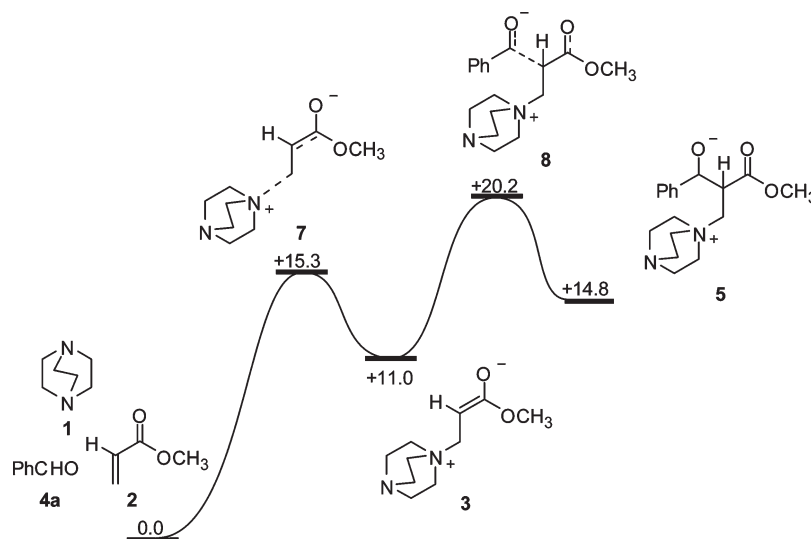
(29) (a) Herrero, M. A.; Kremsner, J. M.; Kappe, C. O. *J. Org. Chem.* **2008**, *73*, 36–47. (b) Obermayer, D.; Kappe, C. O. *Org. Biomol. Chem.* **2010**, *8*, 114–121.

(30) Data points were obtained at 80 (8 h) and 90 °C (6 h). These experiments are described in more detail in the Experimental Section and the Supporting Information.

(31) (a) Robinson, J.; Kingman, S.; Irvine, D.; Licence, P.; Smith, A.; Dimitrakis, G.; Obermayer, D.; Kappe, C. O. *Phys. Chem. Chem. Phys.* **2010**, *12*, 4750–4758. (b) Robinson, J.; Kingman, S.; Irvine, D.; Licence, P.; Smith, A.; Dimitrakis, G.; Obermayer, D.; Kappe, C. O. *Phys. Chem. Chem. Phys.* **2010**, *12*, 10793–10800.

**TABLE 1.** Calculated Thermodynamic Properties for the Morita–Baylis–Hillman Reaction of Benzaldehyde (1a) with Methyl Acrylate (2) in the Presence and Absence of an Electric Field (Scheme 2)

electric field strength (V m <sup>-1</sup> )	$\Delta H$ (kcal mol <sup>-1</sup> )	$\Delta S$ (kcal mol <sup>-1</sup> )	$\Delta G$ (kcal mol <sup>-1</sup> )	$K_{\text{eq}}$
	-14.9240	-45.111	-1.4742	12.012
10 <sup>5</sup>	-14.9240	-45.113	-1.4736	12.000

**FIGURE 5.** Energy profile for the formation of the zwitterionic intermediate **5** calculated at the M06-2X/6-311G(d,p) level (kcal mol<sup>-1</sup>).

thermodynamic properties and theoretical equilibrium constants for the MBH reaction of benzaldehyde with methyl acrylate in methanol (Scheme 2) at 298.15 K in the presence and absence of a static electric field with a strength of 10<sup>5</sup> V m<sup>-1</sup>. The observed differences are very small and rule out the possibility of any direct electric field effects (orientation effects) derived from microwave irradiation on the reaction. These theoretical calculations therefore confirm, as has already been discussed by Stuerger,<sup>32</sup> that the electric field in microwave reactors is orders of magnitude too small to influence the thermodynamic properties of a chemical reaction, and therefore makes the existence of nonthermal microwave effects extremely unlikely.

**Pathway Calculations: General Considerations.** The excellent agreement between the computed and experimental thermodynamic properties for the MBH reaction described above and the recently discovered poor performance provided by B3LYP suggest that a computational reinvestigation of the reaction pathway of the MBH reaction utilizing a proper level of theory would be highly desirable. Unfortunately, the time cost for computing at the MP2/6-311+G(d,p) level some of the transition states in the proposed reaction mechanisms is prohibitively expensive. Accordingly, it was necessary to find a suitable DFT method that is able to reproduce, at least qualitatively, the thermodynamics of the MBH reaction with a reasonable time cost. To accomplish this goal we have evaluated the M06-2X<sup>14</sup> method, which has been shown to deliver improved thermodynamics for carbon–carbon bond forming reactions,<sup>15</sup> along with the 6-311G(d,p) basis set,<sup>21</sup> optimizing the geometries including the solvent effects through the SMD solvation approach (using methanol as solvent). This approximation provided reasonably good values for the

thermodynamic properties for the benzaldehyde case of  $\Delta H = -12.7$  kcal mol<sup>-1</sup> and  $\Delta S = -43.54$  cal mol<sup>-1</sup> K<sup>-1</sup>, very close to the experimental and comparable to the MP2 values (see above), in stark contrast with the poor performance obtained through the B3LYP approach, which predicts a value for the reaction enthalpy of  $\Delta H = +1.4$  kcal mol<sup>-1</sup>, which results in  $\Delta G = +14.4$  kcal mol<sup>-1</sup>. To evaluate if this DFT method can also model the effect of the nitro group, we calculated the thermodynamics for the 4-nitrobenzaldehyde reaction, which were found to be  $-15.1$  kcal mol<sup>-1</sup> and  $-46.5$  cal mol<sup>-1</sup> K<sup>-1</sup>, again being very close to the MP2 results (see above). Figure S1 in the Supporting Information compares the performance of MP2 versus M06-2X for the temperature dependence of the free energies in the MBH reaction for benzaldehyde and 4-nitrobenzaldehyde.

**Carbon–Carbon Bond Formation.** All mechanistic proposals for the MBH reaction start with the formation of the intermediate **5** (Scheme 1 and Figure 1). The first step is the reversible Michael addition of the tertiary amine, in this study DABCO (**1**), to methyl acrylate (**2**), with an energy barrier of 15.3 kcal mol<sup>-1</sup>. The formation of the initial zwitterionic intermediate **3** is endothermic by 11.0 kcal mol<sup>-1</sup>. The coupling of **3** with the benzaldehyde is an aldol addition and one of the proposed rate-determining steps (RDS) for the MBH reaction to produce intermediate **5**. The barrier for the formation of **5** is 20.2 kcal mol<sup>-1</sup> with respect to the separated reactants. Figure 5 shows the calculated energy profile for the formation of the intermediates, and Figure 6 the optimized geometry for the key transition state **8**. From this structure there are different proposals for the formation of the MBH adduct **6** (Figure 1), in which the proton transfer pathway is the crucial problem to understanding the overall process.

**Noncatalyzed Proton Transfer.** There are several proposed pathways to accomplish the proton transfer from the carbon

(32) Stuerger, D. In *Microwaves in Organic Synthesis*, 2nd ed.; Loupy, A., Ed.; Wiley-VCH: Weinheim, Germany, 2006; Chapter 1, pp 1–61.

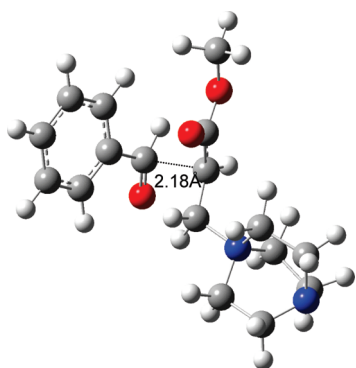


**FIGURE 6.** Optimized geometry for the transition state structure **8**, in one of the plausible rate-determining steps.

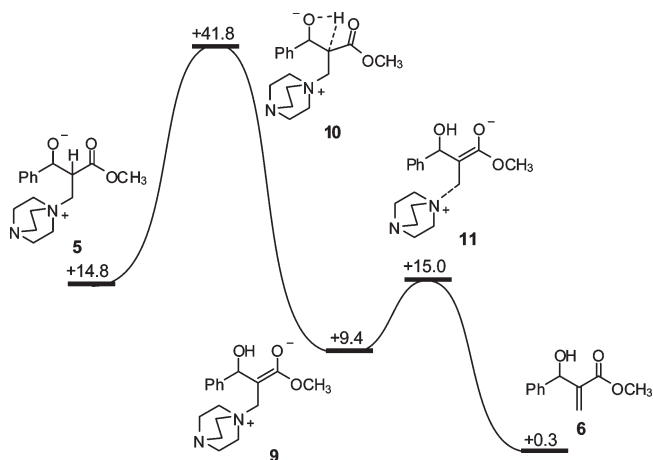


**FIGURE 7.** Energy profile for the direct proton transfer through a 4-membered transition structure calculated at the M06-2X/6-311G(d,p) level (kcal mol<sup>-1</sup>).

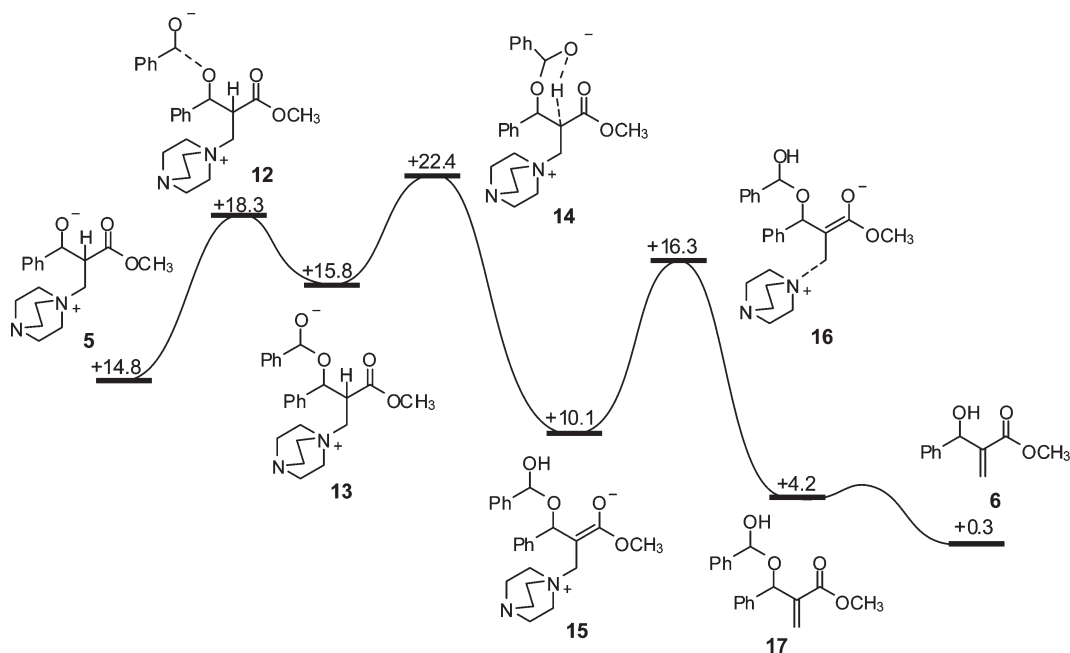
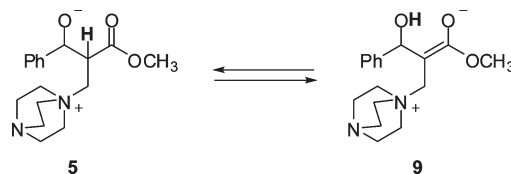


**FIGURE 8.** Energy profile for the 1,3-hydrogen shift and MBH adduct formation via hemiacetal intermediates calculated at the M06-2X/6-311G(d,p) level (kcal mol<sup>-1</sup>).

in intermediate **5** to the oxygen in intermediate **9**, from a direct proton transfer without any assistance via a four-membered ring transition structure, to the aid of a second molecule of aldehyde or a protic species (for example, alcohols, water, or even the MBH adduct).<sup>7,8,16–18</sup>



The direct proton transfer from **5** to form **9** through a four-membered ring transition structure calculated at the M06-2X level has an energy barrier of 41.8 kcal mol<sup>-1</sup> with respect to the separated reactants (Figure 7). This relatively high energy barrier would explain the observed KIE when using isotopically labeled methyl acrylate and the low reaction rates.<sup>7,8</sup> It should be noted that the proton transfer step is exothermic by 5.3 kcal mol<sup>-1</sup>. The intermediate **9** subsequently provides the desired MBH adduct after the release of the catalyst. The elimination of DABCO occurs with an energy barrier of 5.6 kcal mol<sup>-1</sup>, 15.0 kcal mol<sup>-1</sup> with respect to the reactants.

**Reaction in Nonprotic Media.** The kinetic studies of McQuade<sup>7</sup> indicate a second-order reaction for the aldehyde in the absence of other protic species. The previously described proton transfer via a four-membered transition structure cannot explain these experimental observations. Thus, a new mechanism was proposed involving the reaction of intermediate **5** with a second molecule of aldehyde, to form the hemiacetal intermediate **13** (Figure 8). The formation of this intermediate is slightly endothermic by 1.0 kcal mol<sup>-1</sup>, and the energy barrier is only 3.5 kcal mol<sup>-1</sup>, being 18.3 kcal mol<sup>-1</sup> taking as reference the free energy of the reactants. From here, the proton transfer takes place through a six-membered-ring transition structure **14** (Figure 9) with a free energy of activation of 22.4 kcal mol<sup>-1</sup>,

considerably lower than the direct proton transfer mentioned above. In this case the proton transfer is also exothermic by  $5.7 \text{ kcal mol}^{-1}$ . Since this energy barrier is still higher than the carbon–carbon bond formation, this mechanistic proposal explains both the KIE effect and the second-order kinetics for the aldehyde component, agreeing with the previous computational studies by Aggarwal and Harvey.<sup>10</sup> Once the intermediate **15** is formed, the elimination of the catalyst occurs through a relatively low energy transition state, with a relative free energy of  $6.2 \text{ kcal mol}^{-1}$ . The resulting hemiacetal intermediate **17** can

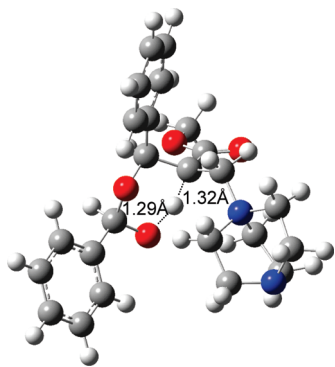


**FIGURE 9.** Optimized structure for the six-membered transition structure **14** proposed by McQuade.

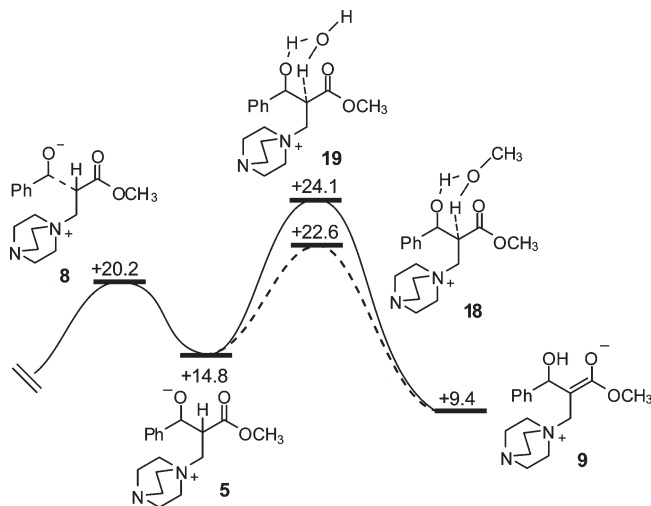


**FIGURE 10.** Energetics of the proton transfer assisted by methanol and water through transition states **18** and **19**, respectively, calculated at the M06-2X/6-311G(d,p) level ( $\text{kcal mol}^{-1}$ ).

then easily decompose to the MBH adduct **6a** and benzaldehyde (**4a**), as previously pointed out,<sup>10</sup> through a series of transition structures involving oxygen–oxygen proton transfers for which no energy barrier was found.

**Reaction Pathway in the Presence of Protic Species.** The well-known acceleration of the MBH reaction in the presence of protic species<sup>1,2</sup> was initially explained by a stabilization of the zwitterionic intermediates (Scheme 1) through hydrogen bonding. However, subsequent studies shed more light on the role of these hydrogen donor structures, presumably being a shuttle for proton transfer.<sup>10</sup> Herein we report the energetics of the alcohol-catalyzed reaction (methanol), along with the assistance of other protic species known to be efficient such as water, phenol, and the MBH adduct itself (autocatalysis).

The methanol-catalyzed proton transfer (Figure 10) has an energy barrier of  $22.6 \text{ kcal mol}^{-1}$ , which is quite analogous to the reaction assisted by a second molecule of aldehyde. These similar energetics can result in competitive reactions, so depending on the amount of protic species and the reaction progress both pathways can take place. When the protic species is water, the energy barrier is slightly higher ( $24.1 \text{ kcal mol}^{-1}$ ). Therefore, the water-assisted hydrogen 1,3-shift will also compete with the second-order aprotic reaction.

The somewhat abnormal kinetic data obtained by McQuade<sup>7</sup> when adding water to the reaction mixture in THF can now be explained when the possibility of competition mechanisms is taken into account. When adding a protic species to the reaction mixture, the authors observed a change in the kinetics, from second order for the aldehyde to an intermediate reaction order (1.4–1.7 for the aldehyde).<sup>7</sup> This was rationalized as being the result of the insolubility of the reactants in the mixture.<sup>7</sup> Assuming that both mechanisms are in fact competing, we fitted the experimental data published by McQuade to eq 2 representing two competitive pathways (Figure 11). Gratifyingly, the correlation coefficients improved appreciably compared to the originally reported values which were calculated assuming a single reaction channel.<sup>7</sup>

$$\frac{\partial[\text{P}]}{\partial t} = k_{\text{aprotic}}[\text{ArCHO}]^2 + k_{\text{protic}}[\text{ArCHO}] \quad (2)$$

Figure 12 shows the variation of the experimental kinetic constants with the addition of different amounts of water. With low amounts of the protic solvent (approximately 0.08 M) the protic pathway rate constant is close to zero, as expected, and the corresponding rate constant for the aprotic pathway is relatively low. When the amount of water is increased both

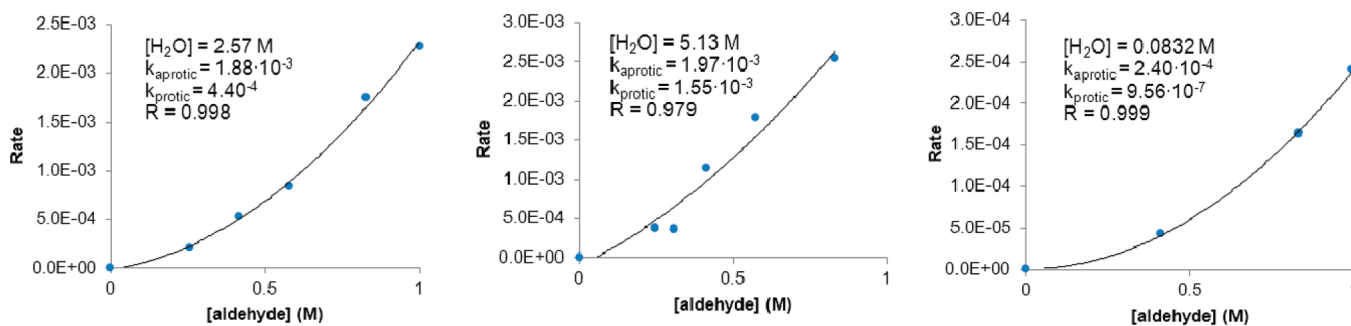


**FIGURE 11.** Reinterpretation of the kinetic data obtained by McQuade assuming two competing mechanisms.<sup>7</sup>



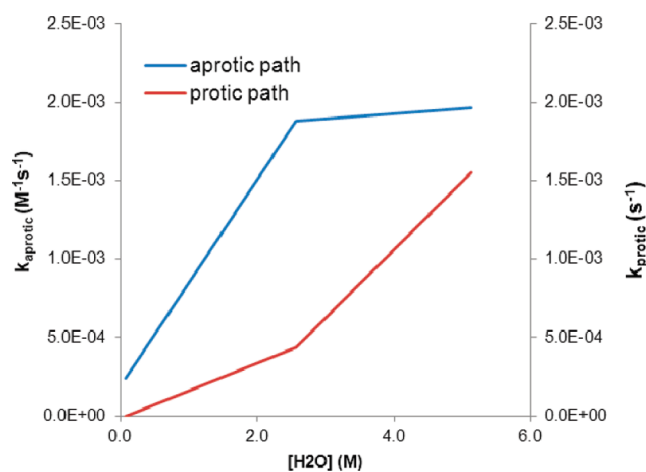


FIGURE 12. Rate constants for the protic and aprotic pathways when increasing the amount of water.

mechanisms increase their speed, while with high amounts of water the aprotic path rate increases slowly and the protic one becomes more significant. Since the kinetic constants have different units they cannot be directly compared, but if we assume, for example, a 1 M concentration of aldehyde at the beginning of the reaction both constants can be put in relation to each other, since in this case the rate constants and reaction rates will be equivalent. Using this assumption it appears that the aprotic pathway is always faster than the reaction assisted by water, as predicted by our DFT calculations (the energy barriers for the proton transfer assisted by the second molecule of aldehyde and water are 22.4 and 24.1 kcal mol<sup>-1</sup>, respectively), and this explains also why the transformation is still second order for the aldehyde even after the addition of water. However, taking into account that the difference is not high ( $\Delta\Delta G^\ddagger = 1.7$  kcal mol<sup>-1</sup>), as the reaction advances, the protic mechanism will become more important and the reaction will not be second order for the aldehyde anymore.

This dualistic nature of the MBH reaction has been previously suggested<sup>10</sup> and experimentally addressed by Eberlin and Coelho.<sup>9</sup> In their experiments, the authors changed the reaction conditions from nonprotic solvent-free to enriched protic conditions by addition of  $\beta$ -naphthol or methanol, and characterized the key intermediates of both pathways by electrospray ionization mass spectrometry. However, no evidence pointing to the fact that both mechanisms can take place simultaneously in a competitive manner has been presented.

It should be noted that, although benzaldehyde has been used as model substrate in our pathway calculations, some of the above-mentioned experiments were carried out with 4-nitrobenzaldehyde and THF–water mixtures as solvent.<sup>7</sup> Therefore, to ascertain that our mechanistic conclusions are also valid for the 4-nitrobenzaldehyde/THF/water system, we have calculated the corresponding energy barriers for the competing mechanisms including the nitro substituent and THF as solvent (the geometries were optimized into the new solvent). Table 2 shows the computed energy barriers. Noticeably, both mechanism have analogous energetics in THF compared to those observed in methanol, both for benzaldehyde, as well as for 4-nitrobenzaldehyde. Thus, it

TABLE 2. Calculated Energy Barriers in THF for the MBH Reaction of Benzaldehyde and 4-Nitrobenzaldehyde with Methyl Acrylate with DABCO as Catalyst, Calculated at the M06-2X Level

substrate	$\Delta G^\ddagger_{\text{aprotic}}$ (kcal mol <sup>-1</sup> )	$\Delta G^\ddagger_{\text{protic}}$ (kcal mol <sup>-1</sup> )
C <sub>6</sub> H <sub>5</sub> CHO	28.9	29.8
4-NO <sub>2</sub> C <sub>6</sub> H <sub>4</sub> CHO	24.5	24.7

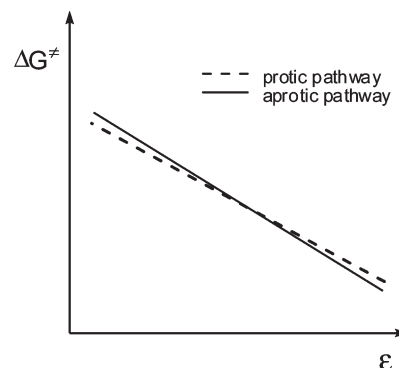
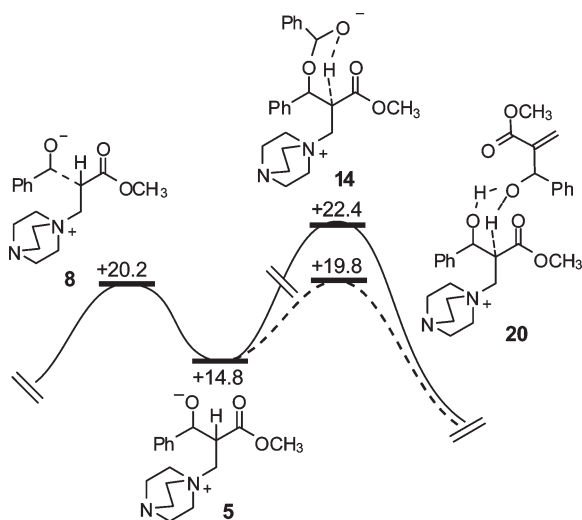


FIGURE 13. Energy barriers for the protic and aprotic pathways vs dielectric constant of the media.

can be assumed that the mechanistic hypothesis about the competitive pathways is also valid when employing different substrates and/or when using a different solvent such as THF. As expected, the energy barriers are lower in the case of the nitro-substituted reactant, with a  $\Delta\Delta G^\ddagger$  of  $-4.4$  and  $-5.1$  kcal mol<sup>-1</sup> for the aprotic and protic pathways, respectively. It is also of interest to note that the energy barriers found in THF are higher in comparison to methanol, for both the aprotic as well as the protic mechanisms. When adding water ( $\epsilon = 78.4$ ) to THF ( $\epsilon = 7.4$ ) in sufficient amount, the dielectric constant of the bulk medium will become intermediate between both solvents and therefore similar to methanol ( $\epsilon = 32.6$ ). In this way the protic and aprotic pathways will become faster. Therefore, our theoretical study can also explain the previously observed acceleration of the MBH reaction when altering the solvent,<sup>1,2</sup> as a result of the change in the dielectric constant of the medium (Figure 13). The choice of reaction pathway will depend on the amount of protic species and the progress (early or late stage) of the reaction.

Even in the absence of any protic species in the reaction medium, a second-order kinetics for the aldehyde is observed only at the initial stages of the reaction. After approximately 20% conversion it is supposed that autocatalysis must take place.<sup>8</sup> However, the proton transfer assisted by a protic species has a similar energy barrier as the second-order mechanism (i.e., assisted by a second molecule of aldehyde), being even slightly higher in the case of water. To explain this point the assistance of the OH group in the MBH adduct must be more efficient than considering the OH group in methanol or water. The calculation of the energetics of this proton transfer step is therefore crucial for the mechanistic understanding of the MBH pathway. Figure 14 shows the different energetics for the proton 1,3-shift in both pathways. The autocatalyzed mechanism has a lower energy barrier by 2.6 kcal mol<sup>-1</sup> with respect to the aprotic path, becoming even slightly lower than that for carbon–carbon bond formation. Taking into account these energetics, the autocatalyzed pathway will have the leading role after approximately



**FIGURE 14.** Energy profiles for the proton transfer catalyzed by a second molecule of aldehyde and the hydroxyl group of the reaction product **6a** calculated at the M06-2X/6-311G(d,p) level ( $\text{kcal mol}^{-1}$ ). Interestingly the autocatalyzed free energy of activation becomes lower than for carbon–carbon bond formation. The geometry of the transition state **20** is shown in Figure 15.

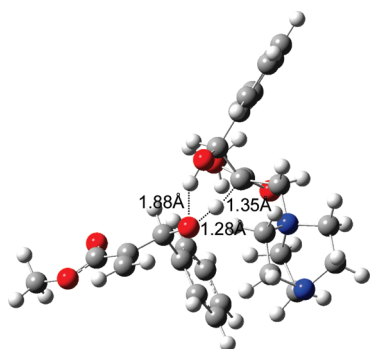


**FIGURE 15.** Optimized geometry for the transition state **20** involved in the autocatalyzed proton transfer.

20% conversion, and therefore the second-order kinetics is only observed at the early stage of the reaction. Again, these computational results nicely fit the experimental observations for the MBH reaction mechanism.<sup>7,8</sup>

Another interesting recent observation in the MBH reaction that has not been clarified from a mechanistic point of view is the substantial rate improvement when using aromatic alcohols (e.g., phenol) as additives,<sup>18</sup> which suggests that the aromatic character of this protic species must be important in the proton-transfer assistance. To substantiate this hypothesis we have additionally calculated the energetics of the proton transfer in the presence of phenol. Noticeably, the energy barrier is significantly lower compared to that of all alternative computed pathways (see above),  $16.1 \text{ kcal mol}^{-1}$  (Figure 16), and also considerably lower than the carbon–carbon bond formation to provide intermediate **5**. Thus, in the presence of phenol the RDS of the MBH reaction changes, and therefore using this additive will result in a significantly faster process as compared to other protic additives such as methanol or water.

It should be noted that in the pathways catalyzed by protic species, after the proton transfer the resulting intermediate **9**

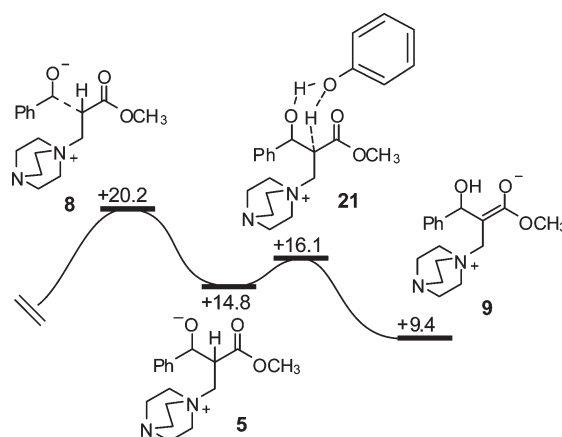


**FIGURE 16.** Calculated energy profile for the proton transfer in the presence of phenol calculated at the M06-2X/6-311G(d,p) level ( $\text{kcal mol}^{-1}$ ).

will evolve to the MBH adduct **6** and DABCO in the same way as in the case of the noncatalyzed reaction.

The different steps for the formation of adduct **6** through all the described reaction channels involve associative and dissociative steps. Therefore, the changes in the system entropy could play an important role when comparing these transformations. However, it should be noted that for the different catalytic cycles the same number of molecules are gathered in the key transition structures, which should lead to similar activation entropies. For example, if we compare the reaction assisted by water, methanol, phenol, or the autocatalysis, in all the cases four particles are associated from the reactants (DABCO, acrylate, aldehyde, and the protic species). The calculated activation entropies for these examples are analogous, even more unfavorable for the phenol assisted and autocatalyzed transformations in comparison with the water and methanol accelerated proton migrations. Thus, the enthalpy must play the leading role in the differences observed in free energies of activation calculated for all the mechanisms.

## Conclusion

In summary, we have performed a detailed investigation on the thermodynamics of the Morita–Baylis–Hillman reaction in order to understand the nature of the reaction equilibrium. Because of the observed enthalpy and the entropy of the reaction, obtained by accurate ab initio MP2 computational methods and verified by variable-temperature measurements of the equilibrium constant, the reaction shifts from exergonic to endergonic when heated at temperatures above  $\sim 57^\circ\text{C}$  in the case of the benzaldehyde/methyl acrylate system. The temperature for this equilibrium reversal is higher for 4-nitrobenzaldehyde ( $\sim 107^\circ\text{C}$ ), due to the higher reaction exothermicity, accounting for the possibility of reaction enhancement at higher reaction temperatures for this substrate.

The reaction mechanism has been subjected to an in-depth computational analysis, employing the M06-2X density-functional method, which has demonstrated superior performance compared to the standard B3LYP protocol. While the M06-2X approach provides values for the reaction enthalpy and entropy in quite good agreement with the experimental and

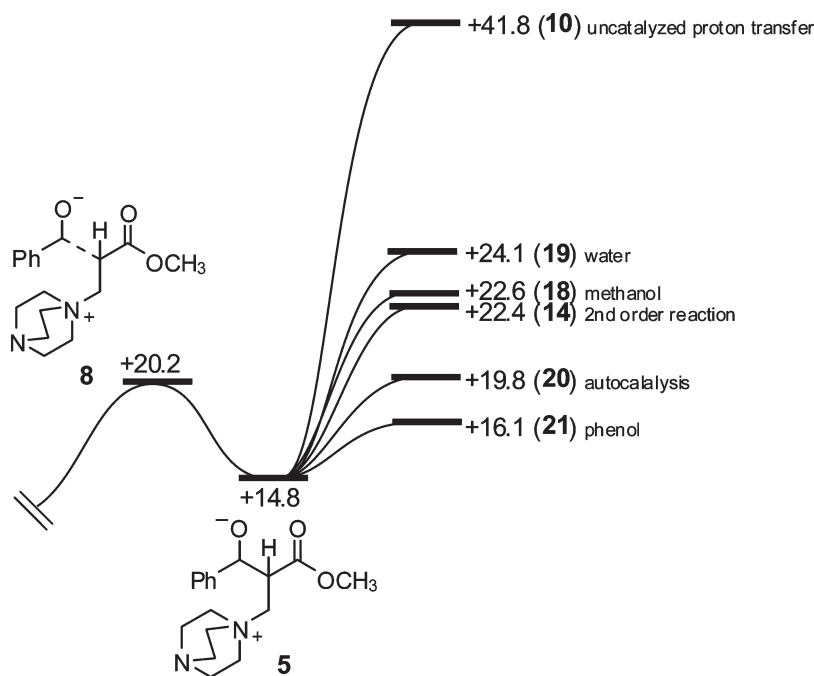


**FIGURE 17.** Energetic summary for all the computed pathways for the proton migration step **5** → **6** (M06-2X/6-311G(d,p) level, kcal mol<sup>-1</sup>).

MP2 results ( $\Delta H = -12.7$  kcal mol<sup>-1</sup> and  $\Delta S = -43.54$  cal mol<sup>-1</sup> K<sup>-1</sup>), the B3LYP method provided very poor results for computing thermodynamic properties in the MBH reaction. This lack of accuracy is in agreement with the previously reported general poor performance of the B3LYP method in modeling energy barriers for the MBH reaction.<sup>11</sup> The complete reaction pathway—including the different proposals for the controversial proton migration step—has been computed. The achieved energetics along with a reinterpretation of the available kinetic data have allowed us to arrive at the conclusion that the McQuade and Aggarwal mechanistic proposals (Figure 1) are in fact competing mechanisms, as demonstrated by the similar computed energy barriers of 22.4, 22.6, and 24.1 kcal mol<sup>-1</sup> for reactions in aprotic media, or catalyzed by methanol and water, respectively (Figure 17). These conclusions have been corroborated by a reinterpretation of the available kinetic data<sup>7</sup> assuming the possibility of two reaction channels. The fitting of the experimental kinetics when adding water with this new hypothesis shows a very good correlation, improving on the previously described data<sup>7</sup> taking into account only one reaction channel. Depending on the amount of protic species and the reaction progress (early or late stage) both pathways can be in operation. In addition, other experimental features of the MBH reaction have been computed (Figure 17), such as the importance of rate acceleration in the presence of aromatic alcohols (phenol), which shows a significant decrease in the computed energy barrier, 16.1 kcal mol<sup>-1</sup>, more than 6 kcal mol<sup>-1</sup> below the above-mentioned energetics. The observed autocatalysis can also be adequately computed by using the M06-2X density-functional method. Thus, the hydrogen migration assisted by the MBH adduct itself (**6a**) shows an energy barrier of 19.8 kcal mol<sup>-1</sup>, significantly lower in comparison with the assistance of a second molecule of aldehyde, and explaining the experimental observation of second-order kinetics in the early stage of the reaction.

The experiments and accurate calculations on the MBH reaction presented herein therefore resolve the remaining open questions regarding the reaction mechanism of this important synthetic transformation.

## Experimental Section

**Microwave Irradiation Experiments and Reaction Monitoring.** Microwave irradiation experiments were performed with a Monowave 300 single-mode microwave reactor from Anton Paar GmbH (Graz, Austria).<sup>28</sup> The reaction temperature was monitored by an internal fiber-optic temperature probe (ruby thermometer) protected by a borosilicate immersion well inserted directly into the reaction mixture. The precision of the internal temperature measurement was provided by efficient stirring at a fixed rate of 600 rpm. GC-FID analysis was performed on a standard GC instrument with a flame ionization detector, using a HP5 column (30 m × 0.250 mm × 0.025 mm). After 1 min at 50 °C the temperature was increased in 25 deg min<sup>-1</sup> steps up to 300 °C and kept at 300 °C for 4 min. The detector gas for the flame ionization is H<sub>2</sub> and compressed air (5.0 quality). Anhydrous solvents (stored over molecular sieves) and chemicals were obtained from standard commercial vendors and were used without any further purification.

**Equilibrium Constant Measurements.** To a solution of methyl acrylate (0.450 mL, 5.0 mmol) in methanol (4 mL) was added DABCO (560 mg, 5.0 mmol), and the corresponding aromatic aldehyde (5.0 mmol). After stirring the volume of the reaction mixture was measured to be 5.4 (for benzaldehyde) and 5.5 mL (for 4-nitrobenzaldehyde), respectively. The reaction mixture was either placed in a sealed Pyrex screw cap reaction vial and heated on a hot plate equipped with a silicon carbide heating block with a 6 × 4 deep well matrix,<sup>33</sup> or irradiated in the microwave instrument at the desired temperature. The reaction progress was monitored by GC-FID injecting samples of approximately 2 μL and diluted in acetonitrile.

(33) (a) Damm, M.; Kappe, C. O. *Mol. Diversity* **2009**, *13*, 529–543. (b) Damm, M.; Kappe, C. O. *J. Comb. Chem.* **2009**, *11*, 460–468.

**Acknowledgment.** This work was supported by a grant from the Christian Doppler Research Society (CDG). D.C. thanks the Spanish Ministerio de Educación y Ciencia for a fellowship and the Fundación Computación y Tecnologías Avanzadas de Extremadura (COMPUTAEX) for computing resources.

**Supporting Information Available:** Equilibrium constant and microwave heating details, complete ref 16, stereoisomeric

pathway descriptions, images of transition state structures, Cartesian coordinates, energy, and imaginary frequency (transition states) for all the calculated stationary points. This material is available free of charge via the Internet at <http://pubs.acs.org>.

**Note Added after ASAP Publication.** Figure 1 was replaced in the version reposted on November 22, 2010.